# Electrochemical Oxidation of Elemental Indium in Liquid Ammonia Media*

**(the late) Theodore A. Annan, Jiansheng Gu, Zhigang Tian and Dennis G. Tuck**
*Department of Chemistry and Biochemistry, University of Windsor, Windsor, Ontario N9B 3P4, Canada*

The electrochemical oxidation of indium metal in solutions of $NH_4X$ (X = Cl, Br or I) in liquid ammonia proceeds with an electrochemical efficiency which implies the formation of indium(II) species at the anode. In the case of $NH_4I$–$NH_3$, Raman spectroscopy confirmed the presence of $In_2I_4$ in solution; it was not possible to isolate neutral or anionic derivatives of indium(II), since disproportionation occurs on removal of solvent to give indium-(0), -(I) and -(III) derivatives. Mass-balance experiments have been made for these systems. Solutions of $NH_4I$ + substituted *o*-quinone ($Bu^t_2H_2C_6O_2$-*o* or $Br_4C_6O_2$-*o*) yielded $InI_3{\cdot}3NH_3$, while with substituted catechols [$X_4C_6(OH)_2$; X = Cl or Br] the products were $[NH_4]_3[In(O_2C_6X_4)_3]{\cdot}Et_2O$. In the case of a solution of $Bu^t_2H_2C_6(OH)_2$-*o* ($H_2$dbc) in liquid $NH_3$–$Et_2O$ media, the final product is a derivative of the dimeric anion $[In_2(dbc)_4(NH_3)_2]^{2-}$, in a lattice which also contains $NH_4^+$, $Hdbc^-$ and $Et_2O$. The crystal parameters of $[NH_4]_4[In_2(dbc)_4(NH_3)_2]{\cdot}(2Hdbc){\cdot}2Et_2O$ are monoclinic, space group $P2_1/n$, $a = 14.464(10)$, $b = 19.194(5)$, $c = 19.560(7)$ Å, $\beta = 103.72(4)°$, $Z = 4$, $R = 0.055$. The anion involves two $InO_5N$ kernels, with $In_2O_2$ cross-linking responsible for the dimerization.

The electrochemical oxidation of a sacrificial metal anode in non-aqueous solutions of an appropriate ligand, or ligand precursor, has formed the basis of a number of direct syntheses of inorganic and organometallic complexes which have been described in papers from this laboratory. A particularly important conclusion is that the product is frequently that of the metal in a low oxidation state; examples relevant to the present paper include $Sn(O_2R)$,[1] $In[O(OH)R]$,[2] $In[S(SH)R]$,[3] $Cu_2[O(OH)C_6Cl_4]_2{\cdot}dppe$[4] and $Pb(O_2R)$[5] (R = aromatic or alkyl group, dppe = $Ph_2PCH_2CH_2PPh_2$). The facile preparation of such compounds has led to the study of their oxidative-addition reactions with iodine, and with substituted *o*-quinones.[1,2,5] These results, together with other current work on the preparation and properties of indium-(I) and -(II) compounds, prompted us to re-examine the work of McElroy, Kleinberg and Davidson[6,7] on the electrochemical oxidation of gallium and indium in liquid ammonia media. These authors reported an electrochemical efficiency ($E_F$, defined as moles of metal dissolved per Faraday of charge) and other results, implying the formation of gallium(II) and indium(II) species, but were unable to isolate any corresponding reaction products. We have confirmed these results in the case of indium, and have also investigated the decomposition of the solution-phase species. Further reactions were carried out with solutions of substituted *o*-quinones or $R(OH)_2$ (R = substituted aromatic), in the hope of stabilizing an indium(II) compound, but in the event we isolated derivatives of $[In(O_2R)_3]^{3-}$ and a crystal structure determination on one such product showed the presence of an interesting novel dimeric anion.

## Experimental

Indium metal (99.99% purity, Aldrich) was used in the form of a rod. Ammonium salts ($NH_4X$; X = Cl, Br or I) and $NEt_4Br$ were dried for 24 h at 110 °C. Organic solvents were dried and distilled before use. Ammonia was supplied as the anhydrous gas, and was further dried by being passed through a tower packed with soda lime, and then over fresh sodium, before being liquified in a previously dried flask immersed in solid $CO_2$–acetone. All other reagents were used as supplied.

Indium analysis was by atomic absorption spectrophotometry, halogen analysis by the Volhard method, and microanalysis was performed by Guelph Chemical Laboratories. Infrared spectroscopy involved the use of samples as KBr or CsI discs, with a Nicolet 5DX instrument. Proton and $^{13}C$ nuclear magnetic resonance spectra were recorded on a Bruker AC 300L spectrometer, electron spin resonance spectra with a Varian E12 instrument, and Raman spectra on a Beckman 700 laser instrument. Conductivity measurements were made with a YSI model 31 bridge, using a conventional cell calibrated with aqueous $KNO_3$ solution.

*Electrochemical Procedures.*—The electrochemical cell was a round-bottomed flask (50 $cm^3$) with a Schlenk arm. The indium rod (2 cm long, diameter 0.5 cm), suspended on a platinum wire through a rubber septum, was the anode of the cell, and a second platinum wire formed the cathode. Prior to electrolysis the indium rod was cleaned with concentrated nitric acid, rinsed with deionized water, dried at 100 °C, and weighed. Dry nitrogen was passed through the flask until all oxygen and traces of moisture had been removed, and the cell was then placed in a cooling bath (solid $CO_2$–acetone) and the appropriate volume of liquid ammonia condensed. The electrical energy was supplied by a Coutant LQ 50/50 power supply, and the total quantity of electricity passed through the cell was determined by means of a silver coulometer in series with the current source, the cell and an ammeter. All experiments were carried out in an inert atmosphere of dry nitrogen. The details of cell composition, electrical conditions and electrochemical efficiency (derived from the weight loss of the anode) are given in Table 1. Typical current densities at the anode were *ca.* 10 mA $cm^{-2}$.

As soon as current flowed in the cell, bubbles of gas were evolved at the cathode. In some cases, small deposition of metal occurred at the anode and/or the cathode, and at the end of the electrolysis this material was filtered off, washed carefully with liquid ammonia, dried *in vacuo*, and weighed. Details of the identification of the particular products are given below.

*Solutions of* $NH_4Cl$.—The surface of the indium anode blackened as the current flowed, and a small quantity of black

---

* *Supplementary data available:* see Instructions for Authors, *J. Chem. Soc., Dalton Trans.*, 1992, Issue 1, pp. xx–xxv.

**Table 1** Experimental conditions and results for halide systems

| Amount of solute (g) | Volume of solvent ($cm^3$) | Initial voltage (V) and current (mA) | Electrolysis time (h) | Mass of In dissolved (mg) | $E_F$/mol $F^{-1}$ |
|---|---|---|---|---|---|
| $NH_4Cl$ (0.39) | $NH_3$ (60) | 6, 20 | 3.0 | 123 | 0.48 |
| $NH_4Br$ (1.02) | $NH_3$ (60) | 5, 20 | 5.0 | 230 | 0.51 |
| $NH_4Br$ (0.17) + $NEt_4Br$ (0.37) | $NH_3$ (60) | 20, 20 | 5.0 | 220 | 0.51 |
| $NH_4Br$ (0.74) + tmen (0.77) | $NH_3$ (60) | 4, 20 | 2.75 | 123 | 0.52 |
| $NH_4I$ (0.80) | $NH_3$ (60) | 4, 20 | 4.0 | 181 | 0.52 |
| $NH_4I$ (0.82) + tmen (0.31) | $NH_3$ (60) | 4, 30 | 4.0 | 160 | 0.50 |
| $NH_4I$ (0.80) + tmen (0.30) | $NH_3$ (30) + MeCN (30) | 3, 20 | 5.0 | 221 | 0.51 |
| $NH_4I$ (0.49) + 18-crown-6 (0.23) | $NH_3$ (30) + MeCN (30) | 4, 20 | 4.75 | 198 | 0.49 |
| $NH_4I$ (0.76) | $NH_3$ (30) + $CH_2Cl_2$ (30) | 5, 20 | 4.0 | 176 | 0.51 |
| $NH_4I$ (0.65) + $NMe_3PhI$ (0.58) | $NH_3$ (60) | 4, 20 | 4.5 | 192 | 0.50 |

solid fell to the bottom of the flask. The current also dropped gradually, and it was necessary to increase the voltage from the initial 6 to about 20 V to maintain a significant current. The black solid was collected and weighed (45 mg); it dissolved in dilute HCl solution, releasing $H_2$, and was identified as indium metal. A portion of the liquid ammonia solution was examined at the end of the electrolysis by Raman spectroscopy, but no significant peaks were found. This system was not studied further.

*Solutions of* $NH_4Br$.—A blue-green coloration was observed near the cathode when current was first passed through the solution. Small black particles subsequently formed, and some black solid was observed on the surface of the indium rod after about 1 h. These black solids were collected, weighed (80 mg), and identified as indium.

In a later experiment, $NEt_4Br$ was added to the solution phase, without substantially changing the course of the reaction. When *N,N,N′,N′*-tetramethylethane-1,2-diamine (tmen) was added, the current dropped gradually during the electrolysis and a gray solid formed on the anode. This solid was subsequently collected, washed with liquid ammonia (2 × 5 $cm^3$), and weighed (50 mg). When a portion of the electrolyte was evaporated, a white solid precipitated, and was collected, dried *in vacuo*, and weighed (119 mg). Analytical results identified this as $InBr_3{\cdot}3NH_3$ (Found: Br, 58.2; In, 28.0. Calc.: Br, 59.1; In, 28.3%). The infrared spectrum confirmed the presence of $NH_3$.

*Solutions of* $NH_4I$.—In addition to the mass-balance investigations described below, we investigated solutions of $NH_4I$ + tmen and $NH_4I$ + $NMe_3PhI$, without producing results qualitatively different from those reported above; this quaternary salt was chosen because its solubility in liquid ammonia (1.80 g per 100 $cm^3$) is higher than that of the other salts examined. Solutions of $NH_4I$ and tmen in liquid $NH_3$ + MeCN were also used, in the hope of precipitating some intermediate product, but here, and in the case of solutions of $NH_4I$ + 18-crown-6 (1,4,7,10,13,16-hexaoxacyclooctadecane), the only solid which could be collected and identified was indium metal. The presence of $CH_2Cl_2$ in $NH_4I$ solutions, added in the hope of generating In–$CH_2$–In species,[8,9] was equally ineffective in changing the course of the reaction.

*Mass-balance Experiments*.—In an attempt at understanding the solution-phase processes in these reactions, we carried out experiments in which each product was weighed and analysed. In the first of these, $NH_4Br$ (1.02 g, 10.44 mmol) in liquid $NH_3$ consumed 0.230 g (2 mmol) of indium over 5 h. The small quantity of black material adhering to the cathode was carefully collected and shown to dissolve completely in dilute HCl with the evolution of $H_2$, and identified as indium metal (0.038 g, 0.33 mmol). A white solid which settled out at the anode was filtered off, washed with liquid $NH_3$, and dried to give a brown solid (mass 0.302 g) (Found: Br, 33.4; In, 39.5%). This analysis corresponds to $InBr{\cdot}4NH_3$ + 0.2 $NH_4Br$ (Calc.: Br, 33.9; In, 40.5%), which accounts for 120 mg In (1.05 mmol) and 101 mg Br (1.26 mmol). The filtrate was allowed to warm up; when the volume had been reduced by *ca.* 70% a white solid precipitated, and was filtered off and dried (mass 0.240 g) (Found: Br, 61.7; In, 24.5. Calc. for $InBr_3{\cdot}3NH_3$ + 0.6 $NH_4Br$; Br, 61.9; In, 24.7%). Total In 58.8 mg, 0.51 mmol; Br 148.1 mg, 1.85 mmol. The final filtrate was taken to dryness, yielding a white solid (0.610 g) containing 1.4% In and 79.0% Br (Calc. for $NH_4Br$: Br, 81.6; In, 0%); Br 482 mg, 6.03 mmol. The total indium recovered in these four solid phases was 0.225 mg, 1.96 mmol, 98% of metal dissolved; for Br, the values are 0.731 g, 9.14 mmol, 88% based on $NH_4Br$ initially present in solution.

Similar results were obtained from an experiment in which indium (0.18 g, 1.58 mmol) was dissolved in a solution containing $NH_4I$ (1.032 g, 7.12 mmol) in liquid $NH_3$ (50 $cm^3$). The black solid (indium metal) recovered from or near the cathode weighed 0.060 g (0.52 mmol). Partial evaporation of the clear electrolyte phase gave a white solid (0.05 g) corresponding to $InI{\cdot}9NH_3$ (Found: I, 34.0; In, 28.5. Calc.: I, 32.1; In, 29.1%). Masses In, 14.3 (0.12); I, 17 mg (0.13 mmol). Evaporation of the filtrate gave 1.05 g of a white solid (Found: I, 74.6; In, 10.0. Calc. for $InI_3{\cdot}6NH_3$ + $4NH_4I$: I, 75.4; In, 9.75%). Masses: In, 105 (0.91); I, 783 mg (6.17 mmol). Total recovered: In, 179 (1.55), 99; I, 800 mg (6.30 mmol), 89%, based on $NH_4I$ dissolved.

*Electrolyses with* 1,2-*Diols*.—The experimental conditions under which these experiments were carried out are shown in Table 2 and the analytical results in Table 3. The important details are given below.

(*i*) Tetrabromocatechol dissolves readily in liquid ammonia to give an orange solution, but electrolysis gave rise to a black solid, identified as indium, which deposited on the surface of the cathode, causing the current to drop gradually. When mixtures of liquid ammonia (30 $cm^3$) and diethyl ether (20 $cm^3$) were used the electrolysis proceeded very smoothly, with no deposition or colour change. At the end of the electrolysis the cooling bath was removed and the liquid ammonia allowed to evaporate gently. After about 4 h, almost all the ammonia had evaporated, leaving the ether, and causing precipitation of a yellow solid, which was filtered off, washed with ether (2 × 5 $cm^3$), dried *in vacuo* and weighed. Analysis identified this compound as $[NH_4]_3[In(O_2C_6Br_4)_3]{\cdot}Et_2O$; the molar conductivity in dimethylformamide (dmf) was 292 $ohm^{-1}$ $cm^2$, slightly higher than the range of 200–240 $ohm^{-1}$ $cm^2$ typically found for 3:1 electrolytes in this solvent at mmol $dm^{-3}$ concentrations.[10] The $^1H$ NMR spectrum in $(CD_3)_2SO$, relative to $SiMe_4$ (δ 0), confirmed the presence of $Et_2O$ (δ 1.10, t; 3.36, q) and $NH_4^+$ (δ 6.7, br); the $^{13}C$ NMR spectrum had resonances at δ 15.2 and 64.9 ($Et_2O$) 107.2 ($C^{4,5}$ of $Br_4C_6O_2^{2-}$), 109.1 ($C^{3,6}$) and 154.7 ($C^{1,2}$) {cf. ref. 11 for comparable values in $[PPh_4][InCl_2(O_2C_6Br_4)]$ and related compounds}. Infrared spectra also demonstrated the presence of $NH_4^+$ and $Br_4C_6O_2^{2-}$ groups in the product.

(*ii*) Electrolysis with pale brown solutions of $Cl_4C_6(OH)_2$ in

**Table 2** Electrochemical conditions for 1,2-diol and *o*-quinone systems

| Solvent volume ($cm^3$) | | | | | | | |
|---|---|---|---|---|---|---|---|
| $NH_3$ | $Et_2O$ | Solute | Mass solute (g) | Initial voltage (V) and current (mA) | Electrolysis time (h) | Mass of In dissolved (mg) | $E_F$/mol $F^{-1}$ |
| 30 | 20 | $Br_4C_6(OH)_2$ | 1.30 | 30, 40 | 2.25 | 136 | 0.35 |
| 30 | 20 | $Cl_4C_6(OH)_2$ | 1.26 | 17, 40 | 3.5 | 193 | 0.32 |
| 30 | 20 | $Bu^t{}_2H_2C_6(OH)_2$ | 1.06 | 35, 40 | 3.3 | 191 | 0.34 |
| 40 | 10 | $NH_4I$ + *o*-$O_2C_{14}H_{20}$ | 0.68 + 0.56 | 3, 22 | 5.25 | 252 | 0.51 |
| 40 | — | $NH_4I$ + *o*-$O_2C_6Br_4$ | 0.57 + 0.74 | 3, 20 | 5.0 | 213 | 0.50 |

**Table 3** Analytical results for catecholato derivatives

| | | Analysis (%)[a] | | | |
|---|---|---|---|---|---|
| Compound | Colour | C | H | N | In |
| $[NH_4]_3[In(O_2C_6Br_4)_3]\cdot Et_2O$ | Yellow | 17.1 (17.5) | 1.60 (1.45) | 3.15 (2.80) | 7.70 (7.60) |
| $[NH_4]_3[In(O_2C_6Cl_4)_3]\cdot Et_2O$ | Pink | — | — | — | 11.7 (11.6) |
| $[NH_4]_4[In_2(dbc)_4(NH_3)_2]\cdot 2Hdbc\cdot 2Et_2O$[b] | Colourless | 61.0 (61.1) | 8.30 (9.15) | 5.30 (4.65) | 12.9 (12.7) |
| $[NH_4]_2[In_2(dbc)_4(dmf)_2]$ | Green | 57.9 (57.6) | 7.53 (7.95) | 5.10 (4.35) | 16.5 (17.8) |

[a] Calculated values in parentheses. [b] After exposure to air, the resultant green crystals had 61.1% C, 7.75% H and 4.70% N.

mixed ammonia–$Et_2O$ media followed the same path, giving $[NH_4]_3[In(O_2C_6Cl_4)_3]\cdot Et_2O$ as the product. The molar conductivity was 214 ohm$^{-1}$ cm$^2$, the $^1H$ NMR spectrum was identical with that of the bromo compound, and the $^{13}C$ NMR spectrum had resonances at δ 15.2 and 64.9 ($Et_2O$), 112.9, 114.5 and 153.2 (*cf.* ref. 11).

(*iii*) Solutions of 3,5-di-*tert*-butylcatechol ($H_2dbc$) in liquid ammonia–$Et_2O$ are extremely air-sensitive, changing from colourless to dark green on exposure to air. The final product of the electrolysis, following work-up as outlined above, was colourless crystals which also turned dark green on exposure to air. These green crystals were paramagnetic. The analysis of this compound, together with the X-ray crystallographic analysis (see below), showed that the lattice is based on a dimeric $[In_2(dbc)_4(NH_3)_2]^{2-}$ anion; in addition to the $NH_4^+$ counter ions, the unit cell also contains $Et_2O$ and $[Hdbc]^-$ (see below), giving the overall elemental composition $C_{92}H_{164}In_2N_6O_{14}$ (see Table 3). In addition to features assigned to $Et_2O$, the $^1H$ NMR spectrum (in $CDCl_3$) had resonances at δ 1.20, 1.34 ($Bu^t$), 3.3–5.1 ($NH_3$, $NH_4^+$) and 6.1–7.8 (aromatic); $^{13}C$ NMR resonances were at δ 29.5, 31.7, 34.3, 35.0 ($Bu^t$), 111.8 ($C^4$), 115.3 ($C^6$), 136.0 ($C^5$), 141.5 ($C^3$), 143.3 ($C^1$ of $Bu_2H_2C_6O_2{}^{2-}$) and 147.9 ($C^2$ of $Bu_2H_2C_6O_2{}^{2-}$) (*cf.* ref. 12). The molar conductivity (mmol dm$^{-3}$ solution) in dmf was 65 ohm$^{-1}$ cm$^2$, typical of a 1:1 electrolyte.

When this compound was dissolved in dmf and recrystallized, the product was $[NH_4]_2[In_2(dbc)_4(dmf)_2]$. The $^1H$ and $^{13}C$ NMR spectra are almost identical to those described above, except for the replacement of $Et_2O$ by dmf [$^1H$ ($CDCl_3$) δ 2.79, 2.88 and 7.88; $^{13}C$ ($C_4D_8O$) δ 35.5, 41.3 and 166.8]. This compound is a non-electrolyte in dmf ($\Lambda_0$ = 5 ohm$^{-1}$ cm$^2$ mol$^{-1}$), which may be due to partial protonation of the $dbc^{2-}$ ligands to give $2NH_3$ + $[In_2(dbc)_2(Hdbc)_2(dmf)_2]$.

*Electrolysis with* o-*Quinones*.—(*i*) There was no spontaneous reaction when indium was immersed in a (yellow) solution of *o*-$O_2C_6Br_4$ in liquid ammonia containing $NH_4I$, and electrolysis proceeded smoothly (see Table 2 for conditions). At the end of the experiment, the black solid deposited around the cathode was filtered off and identified as indium metal (52 mg, 0.45 mmol). Addition of MeCN (60 cm$^3$) to the filtrate precipitated $InI_3\cdot 3NH_3$ (506 mg) which was collected and dried *in vacuo* (Found: I, 68.1; In, 21.6. Calc. for $H_9I_3InN_3$: I, 69.6; In, 21.0%). The mass of indium collected [52 + 109 (0.95 mmol) = 161 mg] is substantially less than that lost from the anode (213 mg, see Table 2), which may be due to the low solubility of $InI_3$ in the solvent mixture.

(*ii*) A similar experiment with a pale yellow solution of 3,5-di-*tert*-butyl-*o*-benzoquinone in liquid $NH_3$–$Et_2O$ led to deposition of shiny indium metal at the cathode. No attempt was made to identify the species present in the solution, which became pink as the electrolysis proceeded.

*Crystallographic Studies*.—A batch of crystals of $[NH_4]_4[In_2(dbc)_4(NH_3)_2]\cdot 2Hdbc\cdot 2Et_2O$ **1** were obtained by electrolysis and evaporation of liquid ammonia. Light mineral oil, which had been degassed by two cycles of freezing and melting *in vacuo*, was syringed into the flask, and individual crystals could then be removed and mounted on a glass fibre with a protective layer of epoxy glue. Under these conditions the crystals remained colourless for up to 3 d; without these precautions they became green during the data collection.

A suitable crystal, an approximately 0.1 mm cube, was mounted in a Rigaku AFC 6S diffractometer, using Mo-K$\alpha$ radiation ($\lambda$ = 0.710 69 Å) and a rotating anode, at 23°. Cell constants, and the orientation matrix, were obtained using 25 machine-centred reflections in the range $25.66 < 2\theta < 29.53°$. From the systematic absences, $h0l$, $h + l \neq 2n$ and $0k0$, $k \neq 2n$, the space group was identified as $P2_1/n$, and this was subsequently taken to be correct in view of the successful refinement. The intensities of three representative reflections measured after every 150 declined by 0.48%, and a linear correction factor was applied. An empirical absorption correction, based on azimuthal scans of several reflections, was applied and resulted in transmission factors ranging from 0.65 to 1.00. The results were also corrected for Lorentz and polarization effects. Pertinent crystal and experimental data are given in Table 4.

The structure was solved by a combination of Patterson and direct methods, with non-hydrogen atoms being refined anisotropically. Hydrogen atoms on carbon were initially included in ideal positions, and subsequently refined isotropically. There is a major problem in identifying two species in the lattice; in addition to the $[In_2(dbc)_4(NH_3)_2]^{2-}$ anion, and its balancing $NH_4^+$ cations, there is a pair of entities which can be written as either ($NH_3$ + $H_2dbc$) or ($NH_4^+$ + $Hdbc^-$). We favour the latter, but decided not to include the hydrogen atoms on nitrogen, or the protonic hydrogens of the 'free' $Hdbc^-$, in the refinement in order not to prejudice these assignments. These units were therefore treated as N and $dbc^{2-}$ respectively. The omitted hydrogen atoms represent a very small fraction of the electron density, and the final *R* value suggests that little was lost by this approach. The programs and other data used are in refs. 13–19.

The convergence minimized the function $\Sigma w(|F_o| - |F_c|)^2$, and in the final cycles the weighting scheme $w = [\sigma(F) + \rho F^2]^{-1}$ was employed, with $\rho = 0.000\,03$. The final atomic coordinates are presented in Table 5, and important interatomic distances and angles of the $[In_2(dbc)_4(NH_3)_2]^{2-}$ anion in Table 6. Fig. 1 shows the structure of this complex, and Fig. 2 shows the arrangement of this and other species in the unit cell.

Additional material available from the Cambridge Crystallographic Data Centre comprises H-atom coordinates, thermal parameters and remaining bond lengths and angles.

## Results and Discussion

*Electrochemistry of* $NH_4X$ *Solutions.*—The results of studies of the electrochemical oxidation of indium in $NH_4X$–liquid ammonia solutions (X = Cl, Br or I) are qualitatively similar to those reported by McElroy *et al.*[6] for $NH_4Br–NH_3$, in that the metal dissolves only when current flows. Quantitatively, there are major differences, primarily in the $E_F$ values, but equally in that we did not observe gas formation at or near to the anode. The electrochemical efficiencies (Table 1) show that for all $NH_4X$ solutions investigated, $E_F = 0.51 \pm 0.01$ mol $F^{-1}$, irrespective of the presence of other solutes, or of organic solvents. In contrast, Kleinberg and co-workers[6,7] reported values (quoted by them as F $mol^{-1}$) which varied between 0.50 and 0.22 mol $F^{-1}$; elimination of these two extremes gives a mean of $0.36 \pm 0.02$ mol $F^{-1}$. The mean oxidation state of the indium species formed is calculated to be $2.44 \pm 0.20$. These authors offered no explanation of the wide variation in their results, but later[7] proposed a mechanism based on the oxidation reactions $In^0 \longrightarrow In^I$ and $In^0 \longrightarrow In^{III}$ in solution, and $NH_3 \longrightarrow N_2 + NH_4^+$ at the anode.

There are no obvious experimental factors on which to base a discussion of the differences between the earlier work and the present results. Given the constant $E_F$ values, and the chemical identification of the indium-(0), -(I) and -(III) species in the final reaction mixture, a reasonable explanation of our results can be based on the sequence of equations (1)–(7).

$$\text{cathode:} \quad 2NH_4^+ + 2e \longrightarrow 2NH_3 + H_2(g) \qquad (1)$$

$$\text{anode:} \quad In + X^- \longrightarrow InX + e \qquad (2)$$

$$InX + X^- \longrightarrow InX_2^- \qquad (3)$$

$$InX_2^- \longrightarrow InX_2^{\bullet} + e \qquad (4)$$

$$2InX_2^{\bullet} \longrightarrow In_2X_4 \qquad (5)$$

$$\text{solution:} \quad In_2X_4 + xNH_3 \longrightarrow InX{\cdot}mNH_3 + InX_3{\cdot}nNH_3 \qquad (6)$$

$$3InX{\cdot}mNH_3 \longrightarrow 2In^0 + InX_3{\cdot}nH_3 + (m-n)NH_3 \qquad (7)$$

The sum of equations (1)–(5) is (8), with $E_F = 0.5$ mol $F^{-1}$.

$$In(s) + 2NH_4X(sln) \longrightarrow 2NH_3(l) + H_2(g) + \tfrac{1}{2}In_2X_4(sln) \qquad (8)$$

The rationale for these proposed processes is based on earlier studies of indium-(I) and -(II), and on the mass-balance studies of $NH_4X–NH_3$ solutions (X = Br or I) described earlier. Ammonium chloride solutions were not investigated, in part because the chemistry of the indium(II)–chloride system is not as well defined as that of the bromide or iodide analogues.[20] The primary process (2), in which $In^IX$ is formed, is in keeping with a number of studies of the electrochemical oxidation of indium in various organic solvent systems, where $E_F = 1.0$ mol $F^{-1}$, and where the InL species subsequently undergoes disproportionation to $In^0$ and $InL_3$, with this latter being the isolated product.[1,2,9,21,22] The formation of $InX_2^-$ species in solution, and in electrochemical synthesis, has been reported previously,[23,24] and liquid ammonia is clearly a medium which supports the formation of low-oxidation-state complexes.[7] The discharge of this anion leads to monomeric $InX_2^{\bullet}$, and this sequence (2)–(4) seems more attractive than one involving the simultaneous discharge of two halide ions [equation (9)]

$$In + 2X^- \longrightarrow InX_2^{\bullet} + 2e \qquad (9)$$

although this also obviously gives $E_F = 0.5$ mol $F^{-1}$. The thermodynamic stability of $InX_2^{\bullet}$, its relation to $In_2X_4$, and the disproportionation of the latter molecules have been discussed elsewhere.[20] In essence, the stabilization of $X_2In–InX_2$ does not depend on the strength of the In–In bond, but rather on the suppression of intramolecular halide transfer, by suitable control of the co-ordinative saturation at indium(II) by strong ligation, and both neutral ($In_2X_4L_2$) and anionic ($In_2X_6^{2-}$) derivatives of $In_2X_4$ are known.[25–28] No $NH_3$ derivatives of indium(II) have been reported. We searched for $In_2X_4$ species in ammonia solution, by Raman spectroscopy; the results were negative for X = Br, but when a solution prepared by electrolysis in $NH_3–NH_4I$ was frozen, sealed into a quartz tube under nitrogen, and examined as a solution, Raman emissions were recorded at 109s, 137m, 153w and 216m $cm^{-1}$. The band at 109 $cm^{-1}$ is assigned as ν(In–In), in agreement with 105 $cm^{-1}$ for $In_2I_4L_2$ compounds, and those at 137 and 153 $cm^{-1}$ as ν(In–I) modes,[26] and there is thus good evidence for the existence of $In_2I_4$ species in this solution. The failure to observe emissions from the bromide system may be due to the lower polarizability of the In–Br bond, or more simply to a lower concentration of $In_2Br_4$ molecules in the solution. Unfortunately, despite this clear evidence of $In_2X_4$ formation in the solution phase, we were not able to prepare adducts with tmen, although this ligand is known to stabilize indium(II) dimers,[26–28] nor were $In_2X_6^{2-}$ anionic complexes obtained when $NR_4X$ salts were present in the electrolyte phase, so that direct oxidation of indium in such solutions is not a synthetic route to indium(II) compounds.

The disproportionation of $In_2X_4$ [equation (6)] is evidenced by the recovery of ammoniates of InX and $InX_3$ (X = Br or I) from the solution. Further disproportionation of InX leads to indium metal and more $InX_3$. If one writes the sequence (10)

$$\begin{tikzcd} 2In \arrow[r] & In_2X_4 \arrow[r] & InX + InX_3 \arrow[d] \\ & & \tfrac{2}{3}In + \tfrac{1}{3}InX_3 \end{tikzcd} \qquad (10)$$

with a fraction $x$ of InX undergoing disproportionation, then $(1 - x)$ mol of InX, $\tfrac{2}{3}x$ mol of In and $\tfrac{4}{3}x$ mol of $InX_3$ should be recovered per 2 mol of In dissolved. For the $NH_4Br$ system this is clearly inadequate, as the mass-balance figures show, and we therefore postulate a further reduction of $InX_3$ at the cathode, with a fraction $y$ of the total $InX_3$ being reduced by a two-electron process which does not affect $E_F$ for the anodic oxidation. Satisfactory agreement with the experimental values is found by taking $x = 0.50$, $y = 0.50$ for $In–NH_4Br$ and $x = 1.00$, $y = 0.10$ for $NH_4I$; see Table 7, which is based upon results in the Experimental section.

The evidence thus far supports the mechanism in equations (1)–(7) and (10), with the important caveat that the mass-balance results refer to processes beyond the electrochemical reactions (*e.g.* removal of solvent by evaporation) and therefore only support the overall nature of this scheme. In particular, no quantitative significance should be ascribed to the values deduced for $x$ and $y$ above, nor should the various ammonia adducts isolated be regarded as unique examples of such complexes.

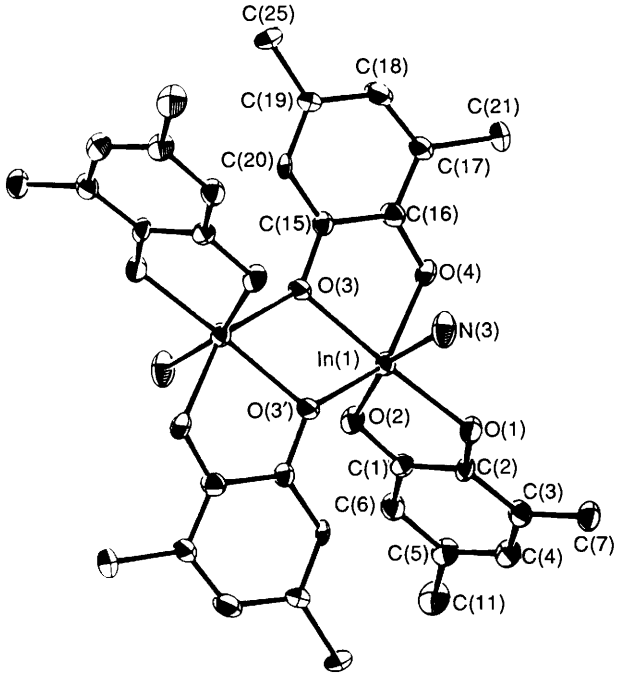

**Fig. 1** The structure of the anion $[In_2(dbc)_4(NH_3)_2]^{2-}$; ORTEP diagram, with atoms represented as 30% probability ellipsoids. Hydrogen atoms have been omitted for clarity

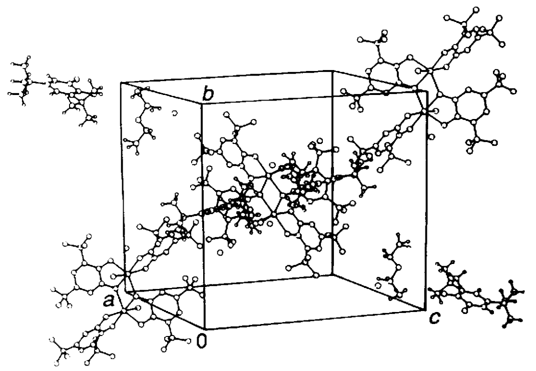

**Fig. 2** Unit-cell diagram of compound **1**, showing $[In_2(dbc)_4(NH_3)_2]^{2-}$, $NH_4^+$, $Hdbc^-$ and $Et_2O$; atoms represented as 20% probability ellipsoids. Hydrogen atoms have been omitted

*o-Quinone Systems*.—The essence of the brief investigation of $NH_4I$–*o*-quinone–liquid $NH_3$ solutions is that $E_F = 0.5$ mol $F^{-1}$, that indium metal is formed at the cathode, and that the only halide isolated is $InI_3{\cdot}3NH_3$. These results are compatible with a scheme in which InI and $InI_3$ are formed in solution as before by equations (1)–(6); in addition to the cathodic reduction of $InI_3$, InI will react with *o*-quinone (*o*-Q) [equation (11)], where $cat^{2-}$ is the diolate anion formed from

$$InI + o\text{-}Q \longrightarrow InI(cat) \qquad (11)$$

the quinone. This oxidation process has been fully discussed elsewhere,[29,30] and is presumably followed by reaction (12).

$$InI(cat) + 2NH_4I \longrightarrow InI_3 + NH_3 + H_2cat \qquad (12)$$

As noted above, the poor mass balance may be due to the finite solubility of $InI_3$ in MeCN.

*Catecholate Systems*.—The presence of an aromatic 1,2-diol in the electrolyte phase, which itself consists of $NH_3$ and $Et_2O$ necessary to bring the diol into solution, adds a further complication to any detailed understanding of an already difficult system. One must presume that the acid–base equilibria (13) and (14) will be established, and may affect other solution-phase

$$NH_3 + H_2cat \rightleftharpoons NH_4^+ + Hcat^- \qquad (13)$$

$$NH_3 + Hcat^- \rightleftharpoons NH_4^+ + cat^{2-} \qquad (14)$$

processes. Furthermore, 1,2-diolates are strong bidentate ligands. The following discussion is based on the assumption that the current carrier and reactive species is the dianion $cat^{2-}$; replacement by $Hcat^-$ increases the number of presumed steps required, but does not change the overall conclusions (see later). The reactions can then be written, by analogy with the above arguments, as in equations (15)–(19). The processes of

cathode: $3NH_4^+ + 3e \longrightarrow 3NH_3 + \tfrac{3}{2}H_2(g) \qquad (15)$

anode: $In + cat^{2-} \longrightarrow In^{II}(cat) + 2e \qquad (16)$

$$In^{II}(cat) + cat^{2-} \longrightarrow [In(cat)_2]^- + e \qquad (17)$$

solution: $[In(cat)_2]^- + NH_4^+ \longrightarrow [NH_4][In(cat)_2] \qquad (18)$

overall: $In + 4NH_4^+ + 2cat^{2-} \longrightarrow [NH_4][In(cat)_2] + 3NH_3 + \tfrac{3}{2}H_2 \qquad (19)$

dimerization and further co-ordination leading to the formation of $[In(cat)_3]^{3-}$ or $[In_2(cat)_4(NH_3)_2]^{2-}$ anions, which are the isolated solid products, are assumed to occur subsequent to equations (17) and (18). The $[In(cat)_3]^{3-}$ products are readily formulated as six-co-ordinate indium(III) complexes, with an $InO_6$ kernel.

As noted in the Experimental section, the lattice of the crystalline product obtained in the case of 3,5-di-*tert*-butylcatechol involves a complex dimeric anion, whose structure is discussed below, diethyl ether, $NH_4^+$, and either $NH_3$ + $H_2dbc$ or $NH_4^+$ + $Hdbc^-$. The latter option seems intuitively the more likely, and may support the presence of $Hdbc^-$, rather than $dbc^{2-}$, anions as the current carriers in the electrolysis. This uncertainty aside, the electrochemical results appear capable of rational understanding, and are in keeping with our present knowledge of indium co-ordination and solution chemistry. The

**Table 4** Summary of crystal data, intensity collection and structure refinement

| | |
|---|---|
| Empirical formula | $(C_{46}H_{82}InN_3O_7)_2$ |
| $M$ | 903.96 × 2 |
| Crystal colour, habit | Pale, blocks |
| Crystal system | Monoclinic |
| Space group | $P2_1/n$ (no. 14) |
| $a$/Å | 14.464(10) |
| $b$/Å | 19.194(5) |
| $c$/Å | 19.560(7) |
| β/° | 103.72(4) |
| $U$/Å³ | 5275(5) |
| $Z$ | 4 |
| $D_c$/g cm$^{-3}$ | 1.123 |
| μ/cm$^{-1}$ | 4.82 |
| $F$(000) | 1936 |
| Scan type | ω–2θ |
| Scan rate/° min$^{-1}$ | 32.0 |
| Scan width/° | 0.89 + 0.30 tanθ |
| $2\theta_{max}$/° | 45.0 |
| Total reflections measured | 7499 (Unique 7166) |
| Unique data used [$I > 3.00\sigma(I)$] | 4147 |
| No. of parameters | 515 |
| $R$ | 0.055 |
| $R'$ | 0.062 |
| Maximum shift/error in final cycle | 0.42 |
| Maximum, minimum (e Å$^{-3}$) in final difference map | 0.98, −0.59 |

**Table 5** Final fractional coordinates for the non-hydrogen atoms of compound **1**

| Atom | *x* | *y* | *z* | Atom | *x* | *y* | *z* |
|---|---|---|---|---|---|---|---|
| In(1) | 0.992 79(4) | 0.089 98(3) | 0.009 42(3) | C(19) | 0.804 9(6) | −0.006 2(5) | 0.167 9(5) |
| O(1) | 0.926 2(4) | 0.175 1(3) | 0.043 0(3) | C(20) | 0.843 3(6) | 0.016 2(4) | 0.115 3(5) |
| O(2) | 1.067 9(4) | 0.094 8(3) | 0.118 9(3) | C(21) | 0.839 9(9) | −0.206 5(6) | 0.154 4(7) |
| O(3) | 0.918 6(4) | −0.007 4(3) | 0.019 7(3) | C(22) | 0.942(1) | −0.231 3(7) | 0.167 6(8) |
| O(4) | 0.906 3(4) | −0.143 0(3) | 0.035 7(3) | C(23) | 0.779(1) | −0.246 6(6) | 0.092 8(8) |
| O(5) | 0.714 2(4) | 0.477 4(3) | 0.691 8(3) | C(24) | 0.803(1) | −0.220 9(6) | 0.217 8(7) |
| O(6) | 0.548 9(5) | 0.529 8(4) | 0.713 7(4) | C(25) | 0.768 2(8) | 0.041 8(6) | 0.216 2(5) |
| O(7) | 0.906 9(9) | 0.371(1) | 0.561 9(7) | C(26) | 0.838(1) | 0.070(2) | 0.266(2) |
| N(1) | 1.226 0(5) | 0.173 1(4) | 0.083 8(5) | C(27) | 0.719(3) | 0.100(1) | 0.178(1) |
| N(2) | 0.195 2(9) | 0.304 4(6) | 0.145 5(7) | C(28) | 0.701(2) | 0.014 9(8) | 0.249(1) |
| N(3) | 0.882 8(5) | 0.105 0(4) | −0.095 6(4) | C(29) | 0.625 9(6) | 0.519 3(4) | 0.771 8(5) |
| C(1) | 1.037 3(6) | 0.150 5(5) | 0.150 4(4) | C(30) | 0.711 6(6) | 0.493 2(5) | 0.759 8(5) |
| C(2) | 0.964 5(6) | 0.192 9(4) | 0.109 8(4) | C(31) | 0.792 5(6) | 0.487 2(5) | 0.815 3(5) |
| C(3) | 0.936 7(6) | 0.253 3(4) | 0.141 6(5) | C(32) | 0.781 5(6) | 0.504 6(6) | 0.881 6(5) |
| C(4) | 0.979 7(7) | 0.266 1(5) | 0.212 6(5) | C(33) | 0.698 6(7) | 0.528 6(5) | 0.895 6(5) |
| C(5) | 1.048 7(7) | 0.223 4(5) | 0.254 2(5) | C(34) | 0.619 6(6) | 0.535 2(5) | 0.838 7(5) |
| C(6) | 1.077 4(6) | 0.165 7(5) | 0.221 1(5) | C(35) | 0.887 0(7) | 0.463 9(6) | 0.802 2(6) |
| C(7) | 0.860 2(7) | 0.301 4(5) | 0.097 2(5) | C(36) | 0.966 2(8) | 0.459 9(8) | 0.871 4(7) |
| C(8) | 0.840 2(8) | 0.364 5(5) | 0.140 9(5) | C(37) | 0.920 7(8) | 0.517 9(8) | 0.755 3(8) |
| C(9) | 0.894 5(8) | 0.329 8(5) | 0.034 7(6) | C(38) | 0.879 8(8) | 0.391 7(7) | 0.770 0(8) |
| C(10) | 0.767 5(7) | 0.263 5(6) | 0.072 0(6) | C(39) | 0.688 1(8) | 0.542 0(6) | 0.972 2(5) |
| C(11) | 1.088 5(9) | 0.237 6(6) | 0.330 5(5) | C(40) | 0.638(1) | 0.480 2(8) | 0.995 1(6) |
| C(12) | 1.061(2) | 0.183(1) | 0.373 6(7) | C(41) | 0.631(1) | 0.607 0(7) | 0.975 6(7) |
| C(13) | 1.059(2) | 0.304(1) | 0.355 8(8) | C(42) | 0.782(1) | 0.550 7(7) | 1.023 5(6) |
| C(14) | 1.191(1) | 0.244(2) | 0.347(1) | C(43) | 0.858(2) | 0.490(1) | 0.541(1) |
| C(15) | 0.877 0(5) | −0.029 3(5) | 0.071 2(4) | C(44) | 0.894(2) | 0.430(2) | 0.515(2) |
| C(16) | 0.873 6(6) | −0.103 1(4) | 0.081 7(4) | C(45) | 0.976(2) | 0.327(2) | 0.551(2) |
| C(17) | 0.838 3(6) | −0.127 9(5) | 0.137 2(5) | C(46) | 0.989(2) | 0.275(2) | 0.605(2) |
| C(18) | 0.803 7(6) | −0.079 2(5) | 0.178 7(5) | | | | |

**Table 6** Selected bond lengths (Å) and angles (°) for the anion $[In_2(dbc)_4(NH_3)_2]^{2-}$

| | | | | | | | |
|---|---|---|---|---|---|---|---|
| In(1)–O(1) | 2.080(5) | C(1)–C(2) | 1.42(1) | C(7)–C(10) | 1.50(1) | C(18)–C(19) | 1.42(1) |
| In(1)–O(2) | 2.161(5) | C(1)–C(6) | 1.40(1) | C(11)–C(12) | 1.45(2) | C(19)–C(20) | 1.35(1) |
| In(1)–O(3) | 2.189(6) | C(2)–C(3) | 1.42(1) | C(11)–C(13) | 1.47(2) | C(19)–C(25) | 1.50(1) |
| In(1)–O(3′) | 2.197(6) | C(3)–C(4) | 1.40(1) | C(11)–C(14) | 1.45(2) | C(21)–C(22) | 1.51(2) |
| In(1)–O(4) | 2.134(6) | C(3)–C(7) | 1.54(1) | C(15)–C(16) | 1.44(1) | C(21)–C(23) | 1.52(2) |
| In(1)–N(3) | 2.299(7) | C(4)–C(5) | 1.39(1) | C(15)–C(20) | 1.39(1) | C(21)–C(24) | 1.49(1) |
| O(1)–C(2) | 1.337(9) | C(5)–C(6) | 1.40(1) | C(16)–C(17) | 1.39(1) | C(25)–C(26) | 1.34(2) |
| O(2)–C(1) | 1.360(9) | C(5)–C(11) | 1.49(1) | C(17)–C(18) | 1.40(1) | C(25)–C(27) | 1.44(2) |
| O(3)–C(15) | 1.355(9) | C(7)–C(8) | 1.55(1) | C(17)–C(21) | 1.54(1) | C(25)–C(28) | 1.39(2) |
| O(4)–C(16) | 1.350(9) | C(7)–C(9) | 1.52(1) | | | | |
| | | | | | | | |
| O(1)–In(1)–O(2) | 79.3(2) | In(1)–O(3′)–C(15) | 111.0(5) | C(3)–C(7)–C(10) | 111.0(8) | C(18)–C(17)–C(21) | 120.9(8) |
| O(1)–In(1)–O(3′) | 111.6(2) | In(1)–O(4)–C(16) | 112.9(5) | C(8)–C(7)–C(9) | 107.6(8) | C(17)–C(18)–C(19) | 123.5(8) |
| O(1)–In(1)–O(3) | 172.2(2) | O(2)–C(1)–C(2) | 118.4(7) | C(8)–C(7)–C(10) | 106.9(8) | C(18)–C(19)–C(20) | 116.8(8) |
| O(1)–In(1)–O(4) | 99.8(2) | O(2)–C(1)–C(6) | 120.6(8) | C(9)–C(7)–C(10) | 110.2(9) | C(18)–C(19)–C(25) | 119.6(9) |
| O(1)–In(1)–N(3) | 84.8(2) | C(2)–C(1)–C(6) | 121.0(8) | C(5)–C(11)–C(12) | 111(1) | C(20)–C(19)–C(25) | 123.6(9) |
| O(2)–In(1)–O(3) | 95.0(2) | O(1)–C(2)–C(1) | 118.9(7) | C(5)–C(11)–C(13) | 115(1) | C(15)–C(20)–C(19) | 122.7(8) |
| O(2)–In(1)–O(3′) | 95.8(2) | O(1)–C(2)–C(3) | 122.9(8) | C(5)–C(11)–C(14) | 111(1) | C(17)–C(21)–C(22) | 108.0(9) |
| O(2)–In(1)–O(4) | 99.0(2) | C(1)–C(2)–C(3) | 118.2(8) | C(12)–C(11)–C(13) | 107(1) | C(17)–C(21)–C(23) | 110(1) |
| O(2)–In(1)–N(3) | 163.5(2) | C(2)–C(3)–C(4) | 118.2(8) | C(12)–C(11)–C(14) | 110(2) | C(17)–C(21)–C(24) | 111.9(9) |
| O(3)–In(1)–O(3′) | 74.8(2) | C(2)–C(3)–C(7) | 118.8(8) | C(13)–C(11)–C(14) | 103(2) | C(22)–C(21)–C(23) | 109(1) |
| O(3′)–In(1)–O(4) | 147.5(2) | C(4)–C(3)–C(7) | 122.9(8) | O(3)–C(15)–C(16) | 116.7(7) | C(22)–C(21)–C(24) | 109(1) |
| O(3′)–In(1)–N(3) | 86.5(2) | C(3)–C(4)–C(5) | 124.3(8) | O(3)–C(15)–C(20) | 123.2(8) | C(23)–C(21)–C(24) | 108(1) |
| O(3)–In(1)–O(4) | 74.8(2) | C(4)–C(5)–C(6) | 116.5(8) | C(16)–C(15)–C(20) | 120.0(7) | C(19)–C(25)–C(26) | 112(1) |
| O(3)–In(1)–N(3) | 100.4(2) | C(4)–C(5)–C(11) | 122.0(9) | O(4)–C(16)–C(15) | 115.7(7) | C(19)–C(25)–C(27) | 111(1) |
| O(4)–In(1)–N(3) | 88.1(3) | C(6)–C(5)–C(11) | 121.5(9) | O(4)–C(16)–C(17) | 125.5(8) | C(19)–C(25)–C(28) | 117(1) |
| In(1)–O(1)–C(2) | 113.2(5) | C(1)–C(6)–C(5) | 121.7(8) | C(15)–C(16)–C(17) | 118.8(8) | C(26)–C(25)–C(27) | 105(2) |
| In(1)–O(2)–C(1) | 110.0(5) | C(3)–C(7)–C(8) | 111.1(8) | C(16)–C(17)–C(18) | 118.1(8) | C(26)–C(25)–C(28) | 108(2) |
| In(1)–O(3)–In(1′) | 105.2(2) | C(3)–C(7)–C(9) | 109.9(8) | C(16)–C(17)–C(21) | 120.9(8) | C(27)–C(25)–C(28) | 103(2) |
| In(1)–O(3)–C(15) | 130.3(5) | | | | | | |

electrochemical route described is at present the only route to these interesting anionic complexes.

*The Structure of* $[In_2(dbc)_4(NH_3)_2]^{2-}$ **1**.—The two indium atoms in this dimer (see Fig. 1) are related by symmetry, each being six-co-ordinate with an $InO_5N$ kernel in which each In–O bond is unique. The average In–O bond distance of 2.152(6) Å is similar to that in $In(acac)Cl_2(bipy)$ (acac = acetylacetonate, bipy = 2,2′-bipyridine)[31] where the average is 2.144 Å, and in $InBr_2(dbsq)(4Me\text{-}py)_2$ (dbsq = 3,5-di-*tert*-butyl-1,2-benzosemiquinonate; 4Me-py = 4-methylpyridine),[30] for which In–O(average) 2.22(1) Å. The shortest In–O bond [In–O(1)] is that *trans* to In–O(3), which involves the bridging oxygen atom, and which is, with In–O(3′), the longest. The

**Table 7** Disproportionation and reduction processes in In–$NH_4X$–liquid $NH_3$ systems (all quantities in mmol)

| X | | In | InX | $InX_3$ | Total In |
|---|---|---|---|---|---|
| Br | Calc. | 0.33 | 1.09 | 0.58 | 2.00 |
| | Found | 0.33 | 1.05 | 0.51 | 1.89 |
| I | Calc. | 0.53 | 0.11 | 0.95 | 1.58 |
| | Found | 0.52 | 0.12 | 0.91 | 1.55 |

In–N(3) bond [2.299(7) Å] can only be compared to those in molecules with bidentate diamine ligands; the average values in indium(III)–tmen systems lie in the range 2.3–2.5 Å, with the actual distances depending strongly on the stereochemistry and the other ligands present.[9,32,33] In sum, the bond lengths are typical of those for octahedral indium(III) species. The bite angles are O(3)–In–O(3′) 74.8(2), O(3)–In–O(4) 74.8(2) and O(1)–In–O(2) 79.3(2)°, to be compared with 74.8(5)° in $InBr_2(dbsq)(4Me\text{-}py)_2$. The other important feature of the bidentate ligand is that the C–O bond lengths are all about 1.35(1) Å, typical of catecholate ligands.

This anion appears to be the first example of a cross-linked $In_2O_2$ dimeric system in which the indium(III) is six-co-ordinate. Two examples of $In_2O_2$ systems based on four-co-ordinate indium are $[InBu^t_2(OEt)]_2$,[34] for which In–O 2.147(5) and 2.165(5) Å, and $[InBu^t_2(OOBu^t)]_2$,[35] in which In–O 2.191(2) Å. These distances are similar to those in the $In_2O_2$ ring of the present complex, In–O(3) 2.189(6), In–O(3′) 2.197(6) Å, despite the different modes of co-ordination. The $In_2O_2$ four-membered ring is clearly an important feature of these molecules, as are $M_2O_2$ and $M_2N_2$ rings (M = Ga or In) in a number of organometallic complexes.[36] The compound $[NH_4]_2[In_2(dbc)_4(dmf)_2]$ is presumably a further example of this structural type, with dmf replacing $NH_3$ in the kernel of six-co-ordinate indium(III). Another related dimeric complex, $In_2(dbc)_2I_2(4Me\text{-}py)_2$ has been obtained in studies of $InI_3$–dbsq$^{\bullet -}$ systems.[37] The structure and properties of this molecule are similar to those of **1**; in particular, both involve $In_2O_2$ cross-linking, and both yield strongly coloured paramagnetic species on dissolution. This latter behaviour will be discussed elsewhere.

## Acknowledgements

This work was supported in part by Operating Grants (to D. G. T.) from the Natural Sciences and Engineering Research Council of Canada. One of us (J. G.) thanks Suzhou University, China, for a leave of absence.

## References

1 H. E. Mabrouk and D. G. Tuck, *J. Chem. Soc., Dalton Trans.*, 1988, 2539.
2 H. E. Mabrouk and D. G. Tuck, *Can. J. Chem.*, 1989, **67**, 746.
3 C. Geloso, H. E. Mabrouk and D. G. Tuck, *J. Chem. Soc., Dalton Trans.*, 1989, 1759.
4 T. A. Annan, J. E. Kickham and D. G. Tuck, *Can. J. Chem.*, 1991, **69**, 251.
5 G. M. Barnard, H. E. Mabrouk and D. G. Tuck, unpublished work.
6 A. D. McElroy, J. Kleinberg and A. W. Davidson, *J. Am. Chem. Soc.*, 1952, **74**, 736.
7 A. W. Davidson and J. Kleinberg, *J. Phys. Chem.*, 1953, **57**, 571.
8 M. A. Khan, C. Peppe and D. G. Tuck, *Organometallics*, 1986, **5**, 525.
9 T. A. Annan, D. G. Tuck, M. A. Khan and C. Peppe, *Organometallics*, 1991, **10**, 2159.
10 W. J. Geary, *Coord. Chem. Rev.*, 1971, **7**, 81.
11 T. A. Annan and D. G. Tuck, *Can. J. Chem.*, 1988, **66**, 2935.
12 T. A. Annan, B. R. McGarvey, A. Ozarowski, D. G. Tuck and R. K. Chadha, *J. Chem. Soc., Dalton Trans.*, 1989, 439.
13 S. Motherwell and W. Clegg, PLUTO, Program for plotting molecular and crystal structures, University of Cambridge, 1978.
14 C. K. Johnson, ORTEP II, Report ORNL-5138, Oak Ridge National Laboratory, Oak Ridge, TN, 1976.
15 J. C. Calbrese, PHASE, Patterson Heavy Atom Solution Extractor, Ph.D. thesis, University of Wisconsin-Madison, 1972.
16 P. T. Beurskens, DIRDIF, Direct Methods for Difference Structures, An automatic procedure for phase extension and refinement of difference structure factors, Technical Report 1984/1 Crystallography Laboratory, Toernooiveld, Nijmegen, 1984.
17 D. T. Cromer and J. T. Waber, *International Tables for X-Ray Crystallography*, Kynoch Press, Birmingham, 1974, vol. 4, Table 2.2A.
18 D. T. Cromer, *International Tables for X-Ray Crystallography*, Kynoch Press, Birmingham, 1974, vol. 4, Table 2.3.1.
19 TEXSAN-TEXRAY Structure Analysis Package, Molecular Structure Corporation, Houston, TX, 1985.
20 D. G. Tuck, *Polyhedron*, 1990, **9**, 377.
21 T. A. Annan, C. Peppe and D. G. Tuck, *Can. J. Chem.*, 1990, **68**, 1598.
22 T. A. Annan, C. Peppe and D. G. Tuck, *Can. J. Chem.*, 1990, **68**, 423.
23 J. J. Habeeb and D. G. Tuck, *J. Chem. Soc., Chem. Commun.*, 1975, 600.
24 J. J. Habeeb and D. G. Tuck, *J. Chem. Soc., Dalton Trans.*, 1976, 866.
25 B. H. Freeland, J. L. Hencher, D. G. Tuck and J. G. Contreras, *Inorg. Chem.*, 1976, **15**, 2144.
26 M. J. Taylor, D. G. Tuck and L. Victoriano, *Can. J. Chem.*, 1982, **60**, 691.
27 I. Sinclair and I. J. Worrall, *Can. J. Chem.*, 1982, **60**, 695.
28 M. A. Khan, C. Peppe and D. G. Tuck, *Can. J. Chem.*, 1984, **62**, 601.
29 T. A. Annan and D. G. Tuck, *Can. J. Chem.*, 1988, **66**, 2935.
30 T. A. Annan, R. K. Chadha, P. Doan, D. H. McConville, B. R. McGarvey, A. Ozarowski and D. G. Tuck, *Inorg. Chem.*, 1990, **29**, 3936.
31 J. G. Contreras, F. W. B. Einstein and D. G. Tuck, *Can. J. Chem.*, 1974, **52**, 3793.
32 M. A. Khan, C. Peppe and D. G. Tuck, *J. Organomet. Chem.*, 1985, **280**, 17.
33 M. A. Khan, C. Peppe and D. G. Tuck, *Organometallics*, 1986, **5**, 525.
34 D. C. Bradley, D. M. Frigo, M. B. Hursthouse and B. Hassan, *Organometallics*, 1988, **7**, 1112.
35 W. M. Cleaver and A. R. Barron, *J. Am. Chem. Soc.*, 1989, **111**, 8966.
36 D. G. Tuck, *Comprehensive Organometallic Chemistry*, eds. G. Wilkinson, F. G. A. Stone and E. W. Abel, Pergamon, Oxford, 1982, vol. 1, p. 683.
37 T. A. Annan, A. Ozarowski, A. El-Hadad and D. G. Tuck, unpublished work.

*Received* 10*th March* 1992; *Paper* 2/01299E